Coupled particle and fluid flow modeling of fracture and slurry injection in weakly consolidated granular media

M.S. Bruno, A. Dorfmann & K. Lao
Terralog Technologies USA, Inc. Arcadia, California, 91006 USA

C.Honeger
University of Applied Sciences, Vienna, Austria

ABSTRACT: Discrete particle models, which simulate inter-particle mechanics explicitly and can be coupled with fluid flow mechanics, often provide a more realistic simulation of granular deformation and fracture than continuum models. We apply such models to investigate fracture processes in weakly cemented media, providing insights on material parameters which influence a change from discrete brittle fracturing (as occurs in stiff and strong geomaterial) to general dilation and parting (as occurs in very soft and weak geomaterials). The primary influence on parting behavior is shear bonding at the granular scale. We also investigate slurry injection processes in granular media by coupling fluid flow simulators with particle models for several near wellbore assemblies. Although there are clear challenges remaining with scaling issues and practical model size, we conclude that coupled particle and fluid flow codes can simulate slurry injection processes well, reproducing dilation and parting patterns consistent with laboratory observations and pressure response consistent with field observations.

1 INTRODUCTION

There are several important petroleum, mining, and environmental engineering applications that involve large-scale deformation, failure, and fluid flow processes in weakly consolidated media. These include gravel injection and "frac-pack" operations to both stimulate a well and provide sanding control, grout injection to create barriers for contaminant flow in porous media, and slurry waste injection in deep wells. Unfortunately, the geomechanical aspects and controls on such operations remain poorly understood. Continuum models have difficulty capturing the basic physical processes of microcracking, disaggregation, and grain movement that occur during fracture and slurry injection in weakly consolidated media. These are inherently "discontinuous" failure processes. Traditional fracture mechanics approaches are particularly ill suited for modeling such phenomena because they are fundamentally based on stress singularities and strain energy dissipation processes at an advancing fracture tip. Fracture or "parting" of weakly consolidated media with near zero shear strength, however, is dominated by energy dissipated deforming, shearing, and dilating material over a large area; fracture toughness and traditional tip mechanics are relatively inconsequential.

The objective of our research, funded in part by the U.S. Department of Energy and the Alberta Department of Energy, has been to develop an improved understanding of such processes by developing alternative modeling techniques. One component of our effort has involved coupled particle and fluid flow modeling.

In this paper we first present an overview of traditional linear elastic fracture mechanics, starting from first energy principles and extending to the stress intensity factor approach common to most hydraulic fracture models. We describe the limitations of such models when considering distributed damage processes involved in fracture and parting of weakly consolidated media, and suggest an alternative approach using discrete particle modeling techniques. We investigate and conclude that particle models can capture observed physical processes in weakly cemented media, providing insights on material parameters which influence a change from discrete brittle fracturing (as occurs in stiff and strong geomaterial) to general dilation and parting (as occurs in very soft and weak geomaterials). The primary influence on parting behavior is shear bonding at the granular scale. Tensile bond properties have much less influence.

Next we investigate slurry injection processes in granular media by coupling fluid flow simulators with particle models for several near wellbore assemblies. Finally, we present simulation results producing dilation and parting patterns consistent with laboratory observations and pressure response consistent with field observations.

2 "FRACTURE" IN GRANULAR MEDIA

2.1 *Linear elastic fracture mechanics background*

The fundamental principles of fracture mechanics are founded on the theoretical and experimental work by Griffith in the 1920s (Griffith, 1921). Starting with the first law of thermodynamics, Griffith postulated that for an increment of crack extension the change in potential energy of deformation must equal the amount of energy required to create the new crack surface. This work was later expanded by Irwin (1948) and Orowan (1948) who recognized that the required energy includes not only surface energy density γ, but also includes dissipative energy d related to microcracking and plastic flow around the tip (which in fact is the larger term for most materials). The resulting failure criteria is expressed in terms of a critical strain energy release rate, Gc (named in Griffith's honor),

$$Gc = dU/dA = \gamma + d \qquad (1)$$

Where dU is the change in internal strain energy and dA is the change in crack surface area.

Irwin (1957) then made the important and critical link between the strain energy release rate, a global energy parameter, and the local stress field and crack opening displacement, using analytical solutions for a cracked body developed by Westergaard (1939). The stresses σ_{ij} and displacements u_i around a crack tip can be expressed in terms of stress intensity factors K for varying fracture modes, and trigonometric relations. For example the Mode I (tensile) stress and displacement fields around the crack tip can be expressed as:

$$\sigma_{ij} = [K/(2\pi r)^{1/2}]\, f_{ij}(\theta) \qquad (2)$$

$$\text{and} \quad u_i = [(K/2\mu)(r/2\pi)^{1/2}]\, g_i(\theta) \qquad (3),$$

where r is the distance to the crack tip, μ is the material shear modulus, and θ is the angle measured from the crack axis. Similar expressions are available for Mode II (in plane shear) and Mode III fracture extension. The stress intensity factor is a function of fracture geometry and load pattern. For a typical Mode I fracture of initial length 2a subject to internal pressure P(x), the stress intensity factor can be expressed as (Rice, 1968):

$$K_I = \frac{1}{\sqrt{pa}} \int_{-a}^{a} p(t) \sqrt{\frac{a+x}{a-x}}\, dx \qquad (4)$$

Because the elastic stress field is singular, there is an inelastic region surrounding the crack tip where failure occurs and the linear elastic solution is not valid. The area outside this region, but for radius still small compared to the overall crack length, is referred to as the K-dominant region in which stresses and displacements may be defined according to equations (2) and (3). This is illustrated schematically in Figure 1. Failure is assumed to occur when the stress field as defined in equation (2) exceeds a critical value expressed in terms of a critical stress intensity factor (fracture toughness) for the material, Kc, within a region around the crack tip.

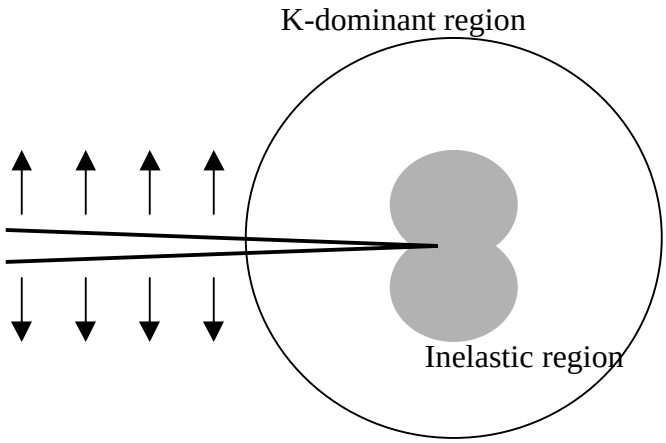

Figure 1. Elastic crack tip stress fields are defined for a K-dominant region surrounding a crack tip and outside a near-tip inelastic zone.

The strain energy release rate in equation (1) may be directly related to the crack tip stress-strain field and stress intensity factors of equations (2) and (3) through virtual work principles. For example, Irwin equated the work done by the near tip stress field acting over the displacement to the product of strain energy release and crack extension increment.

To accommodate the unrealistic development of singular stresses at the tip of a crack, yielded or cohesive stress zones were introduced extending from the crack tip (Dugdale, 1960; Barenblatt, 1962) to model the inelastic response of real materials, as illustrated in Figure 2. Extension of the crack is opposed by a cohesive stress, limited to the yield strength of the material σ_y. The change in strain energy for crack extension may then also be equated to the work done by the yield stress acting over the crack tip opening displacement.

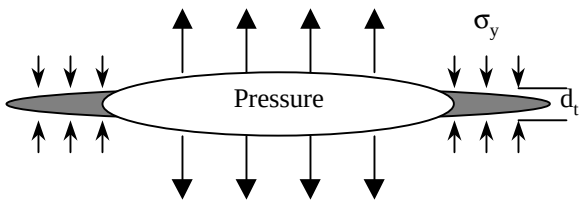

Figure 2. Yielded strip model for crack opening against a given yield stress limit.

For linear elastic bodies, Griffith's energy balance approach, Irwin's stress intensity factor approach, and the Dugdale-Barenblatt crack-tip opening displacement approach to fracture mechanics are all equivalent, and related by:

$$G = dU/dA = (1-\nu^2)K^2/E = \sigma_y d_t \qquad (5)$$

where ν is Poisson's ratio and E is the material Young's modulus. The relations are extended to porelasticity problems by accounting for the additional potential energy associated with pore pressure variations (see for example Cleary, 1979; Bruno & Nakagawa, 1991).

2.2 *Limitations of traditional fracture mechanics to large deformation in granular media*

Expressions (2) through (5) for elastic fracture opening displacements and pressure limits related to critical stress intensity factors and fracture toughness, with modifications to account for fluid flow and leak-off along the fracture length, form the basis for all industry standard hydraulic fracture models and simulators. It is important to recognize the fundamental bases and limitations of such models when considering fracture or parting in weakly consolidated granular media.

To summarize, all modern fracture criteria are fundamentally based on energy balance considerations. This global energy approach has historically been simplified to estimate hydraulic fracture dimensions and pressure limits by considering work done by the elastic stress and strain field around a crack tip as the fracture extends. Standard hydraulic fracture equations are therefore valid only for the following conditions:

1. The size of the inelastic zone surrounding the crack tip is small in comparison to the K-dominant region and the fracture length;
2. Changes in internal strain energy associated with fracture extension are concentrated around the advancing crack tip.

Unfortunately, neither of these conditions are generally valid for fracture injection processes in weakly consolidated media. As pore pressure is increased and effective confining stress decreases in weakly consolidated media, shear strength and tensile strength are essentially zero. The size of the inelastic or plastic zone surrounding a fracture or parting plane is relatively large and not at all confined to the near tip region. Laboratory observations (Willson et al, 1999) and field observations (Bruno et al, 2000) of fracture injection in high permeability media indicate that significant damage and deformation (microcracking, multiple dendritic fracturing, and dilation) occurs along the length of a propagating fracture.

Fracture or "parting" of weakly consolidated media with near zero shear strength, therefore, is dominated by energy dissipated deforming, shearing, and dilating material over a large area; fracture toughness and traditional tip mechanics are relatively inconsequential. These differences are illustrated schematically in Figure 3.

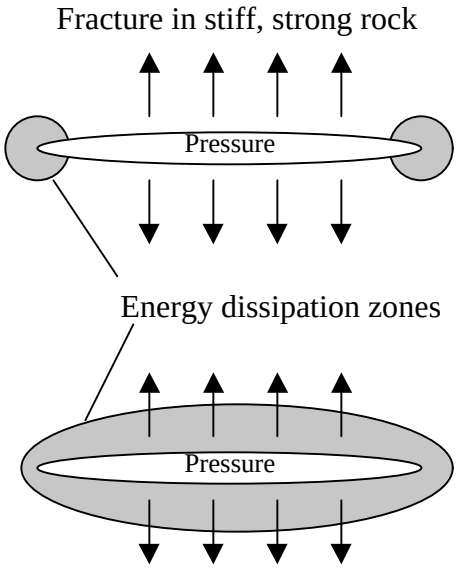

Figure 3. Deformation energy associated with fracture propagation is concentrated at tips in stiff, strong rock, but distributed over larger area in low shear strength granular media.

To properly define the fracture criteria and associated fracture dimensions for weakly granular media, the appropriate energy balance equations must include the change in internal strain energy over the entire area surrounding the fracture or parting zone. We can no longer rely on the elastic solution for stresses and displacements around the crack tip, nor on simplifications related to a single tip fracture extension acting against a given tensile yield stress.

One alternative would be to extend the linear elastic fracture mechanics approach by considering an assumed distribution of tension and shear microcracks at various orientations around the primary parting plane, each with their own stress intensity factors and stress distributions. This becomes extremely problematic for more than a few microcrack extensions, however, and it is clear that continuum elasticity solutions are not appropriate. An alternative approach is to evaluate fracture and parting in weakly consolidated rocks with discrete particle modeling.

3 DISCRETE PARTICLE MODELING

3.1 *Background*

Fracture and dilation of granular media are inherently "discontinuous" processes. Continuum models have difficulty capturing the basic physical processes of microcracking, disaggregation, and grain movement which occurs during slurry injection in weakly consolidated media. Discrete element or particle models, which model interparticle mechanics explicitly, can often provide a more realistic simulation of granular material deformation and flow.

Numerical simulation of cohesionless granular assemblies with discrete elements was introduced by Cundall and Strack (1979), and has since been modified and expanded by a number of researchers. In these models, the movements and mechanical interaction of particles are tracked over time with an explicit finite difference procedure. Particle interaction is modeled by damped force-displacement relations at each contact. The resulting forces and moments are related through Newton's second law to the particle mass and acceleration. Contact forces on the microstructural level may be related to macroscopic boundary stresses through the principal of virtual work, as described by Bathurst and Rothenburg (1990).

Discrete element models for grain assemblies have been applied to investigate stress induced microcracking and induced permeability anisotropy in sandstones (Bruno, 1994) and to investigate sand production around perforations and wellbores (Bruno et al, 1996). Cementation is modeled as tension and shear bonds between grains. Fluid flow can be accommodated explicitly by adding a pore space network flow model to the assembly, solving for the pore pressure field at each time step, and then resolving pressure gradients into body forces at individual grains. Alternatively, a continuum flow model can be run concurrently with the granular model, and using the particle model to update porosity and permeability fields for the flow model.

3.2 *Cementation influence on brittle fracture and dilation*

We first investigate how particle models can capture observed physical processes in weakly cemented media and provide insights on material parameters which influence changes in fracture behavior from discrete brittle fractures (as occurs in stiff formations) to general dilation (as occurs in very soft formations). Figures 4 presents fracture simulations with varying cementation properties. Particles are shown with circles, and contact bonds between particles are shown with dark lines. In each simulation an initial fracture is extended simply by applying normal, outward forces to the starting fracture face, consistent with the forces that would be applied by fluid pressure within the starting fracture. The particle movement and change in contact bond pattern illustrate fracture and deformation patterns resulting from assemblies with varying cementation properties.

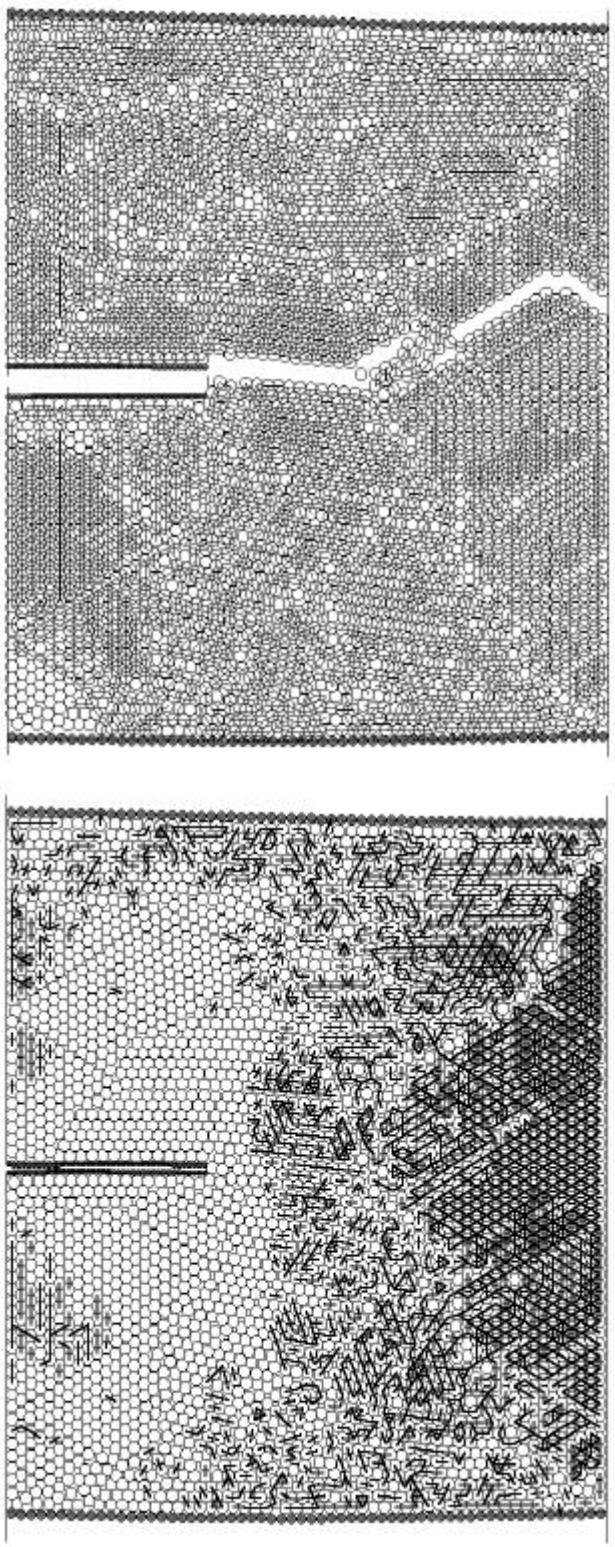

Figure 4. Top figure illustrates brittle single fracture propagation when bond strength is relatively high. Lower figure illustrates general dilation and damage surrounding crack face when shear bond strength is low.

For strongly cemented granular assemblies the fracture propagates in a discrete, brittle manner simply by extending forward. However, for weakly cemented materials (lowermost assembly in Figure 4), deformation is accommodated by general dilation and deformation around the original fracture face, with very limited fracture extension. This transition from brittle fracture extension to general dilation is primarily controlled by shear bonding between particles. That is, a decrease in the shear strength alone between particles produces dilation whereas a decrease in the tensile strength alone does not.

3.3 *Coupled particle and fluid flow simulation*

Next we investigate the process of slurry injection by analyzing the coupled fluid flow and particle mechanics process. In this example we use ITASCA's FLAC program to model fluid flow in a fully saturated media and the PFC program to model particle movement. The general coupling process is illustrated in Figure 5. A Windows interface used to assign properties, call individual subroutines, and track solution progress is illustrated in Figure 6.

To initiate the coupled fluid and particle flow simulation, a matrix of solid particles is first generated with PFC to simulate the weakly cemented sand formation. Neighboring elements in the matrix are connecting by weak bonds, which are allowed to fail upon creation of a limited stress state in the link itself. A corresponding and overlapping FLAC mesh is also generated to model fluid flow, as illustrated in Figure 7.

Porosity values from the particle model shown on the upper image of Figure 7 are used to define an initial permeability field for the fluid flow mesh. In our initial studies, we assume there is a relatively simple relationship between permeability, K, and porosity, ϕ, of the form taken by a Kozeny-Carman equation:

$$K = C\,\phi^{n} \quad , \qquad (6)$$

where the proportionality constant, C, and the exponent, n, are generally related to the specific surface area, grain size, and tortuosity in a granular assembly. In our simulations we use an exponent n=3.0, providing a relatively strong dependency on porosity.

The injection process is simulated by prescribing a flow rate at the borehole and maintaining a constant pressure boundary condition at the outer walls in the model. The assembly is assumed to be completely saturated. For the given initial permeability field and borehole flow rate, FLAC is then run to determine the resulting pore pressure field. For example, Figure 8 presents a sample pressure field determined by the FLAC model.

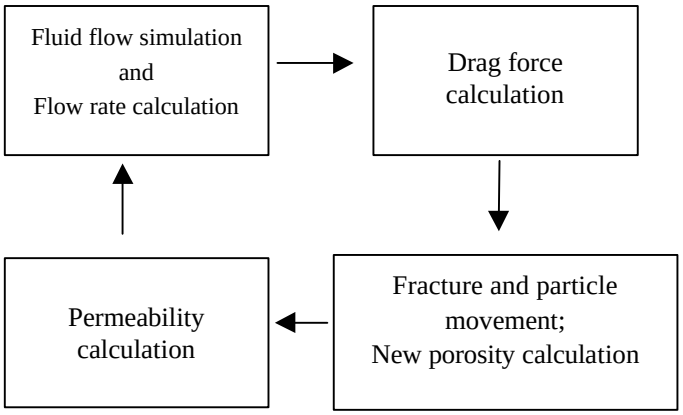

Figure 5. Typical iterative coupling process

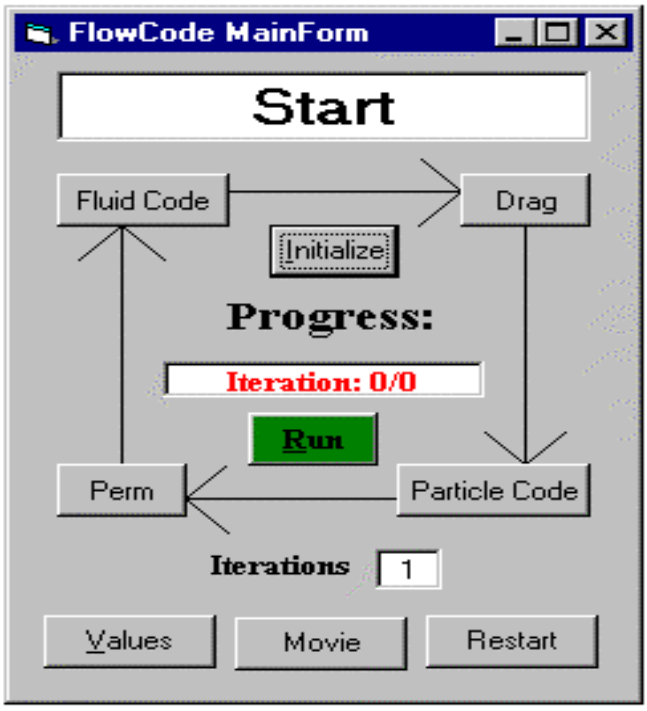

Figure 6. Windows interface developed to couple fluid flow and particle models

The gradient of this pore pressure field, acting in the direction of fluid flow, induces drag forces on the particles. Drag is the resistance to fluid flow posed by the porous matrix (Bear, 1972). The drag force is introduced as an equivalent body force induced by the pressure gradient across the diameter of a particle in the flow direction multiplied by the area of the particle.

$$dF_i = A\frac{\partial P}{\partial x_i} \qquad (7)$$

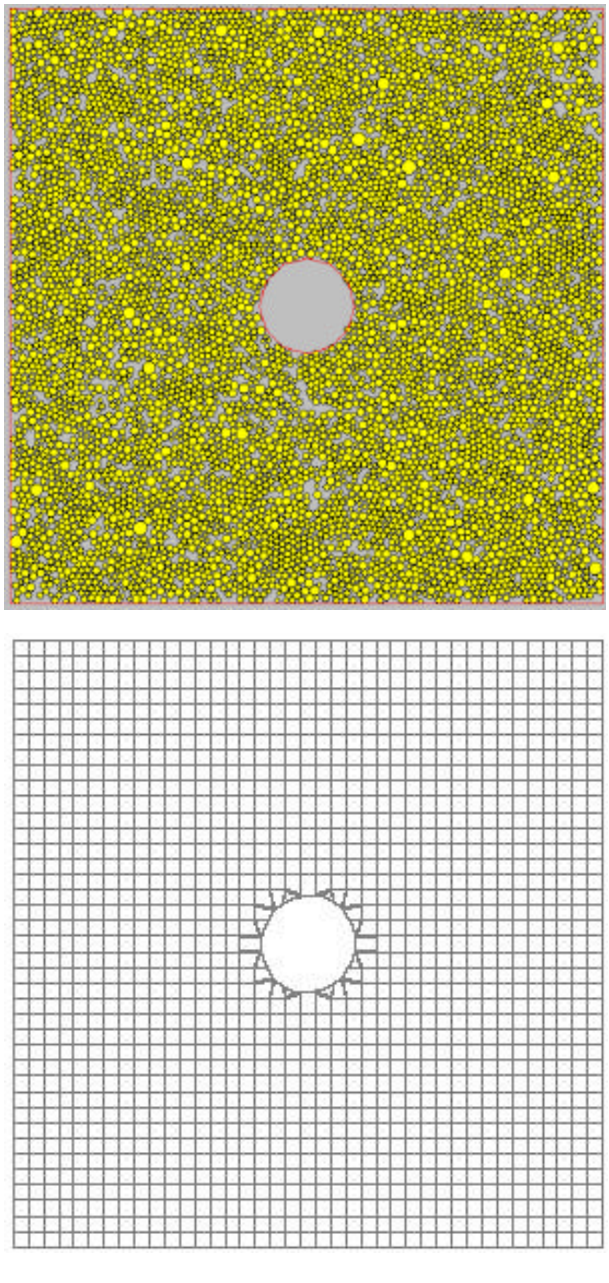

Figure 7. Initial particle mesh assembly (upper figure) and matching fluid flow mesh (lower figure) to simulate slurry injection.

Using the expression for $\partial P/\partial x_i$ from Darcy's equation

$$F = \left(p\, r_g^2\right)\frac{Q}{K}2r_g \qquad (8)$$

where F is the drag force, $\partial P/\partial x_i$ is the geometric pressure gradient in x_i –direction, and r_g is the radius of the grain particle.

At each time step the x- and y-components of this force are added to the total body-force of each particle in the PFC model for the next iteration, and the solution of the equation of motion will then provide new acceleration terms. Time integration results in new values for the vector components of particle velocity, displacement and rotation.

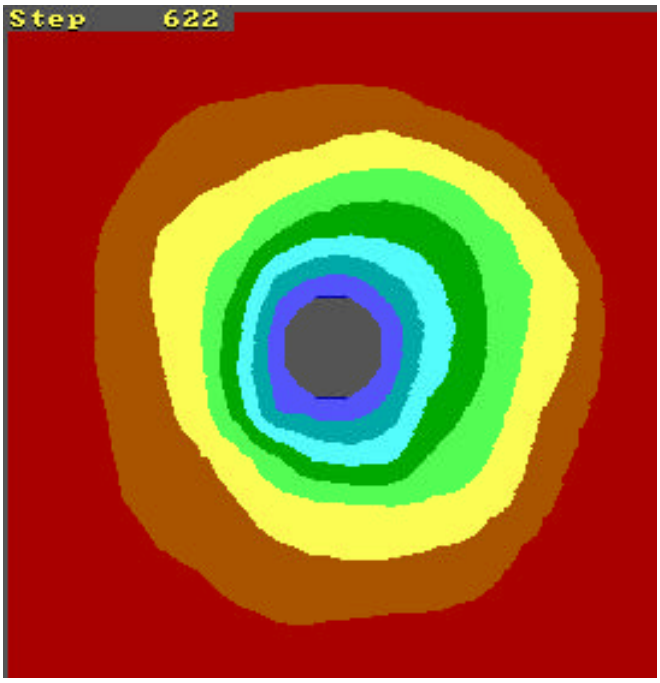

Figure 8. Sample pore pressure distribution in model after several iterations.

Dilation and cracking during this iteration then increases the porosity in a local area around the borehole, and provides new fluid paths that decrease the flow resistance in the porous material. The pressurized fluid in the fracture imposes additional load on the crack faces, thereby wedging the fracture further open. The direction of crack propagation when the porous material is loaded in compression is predominantly parallel to the maximum compressive stress direction.

We introduce slurry particles of a given size into the borehole at a given rate, consistent with the desired density and fluid flow rate. These particles are then swept by the flow field into the matrix and fracture system, contributing to the calculations for determining porosity, drag force, fracturing and fluid flow.

In summary, the iterative fluid flow and geomechanical process proceeds with the following steps:

1. Start with an initial particle assembly and fluid flow mesh, assigning initial material properties;
2. Assign a permeability field to the flow mesh consistent with the initial porosity;
3. Define the desired borehole injection rate, slurry density, and far-field pressure boundary conditions;
4. Run the fluid flow simulator (FLAC) to determine a new pore pressure field;
5. Determine pressure gradients and associated drag forces to be applied to each particle;
6. Run the particle simulator (PFC) to determine deformation in the geomechanical assembly;

7. Calculate the new porosity field and associated permeability field for the assembly;
8. Return to step 4 and iterate again.

3.4 *Simulation results and discussion*

The results of such a simulation are illustrated in Figures 9 through 11. For this simulation displacements are fixed on the lateral boundaries (left and right edges of model), and a fixed compressive stress is prescribed on the vertical boundaries (top and bottom edges). This establishes an anisotropic stress field favoring fracture orientation in the horizontal direction.

First, injection particles (shown in blue) penetrate radially into the matrix. A wide fracture and dilation zone (zone of increased porosity) is initially established by the fluid, which then allows the injected solid particles to enter the fracture and process zone. Solids injection is therefore accommodated not only by fracture creation, but also by the matrix porosity (note penetration of slurry particles into porespace surrounding the borehole). Several fracture branches are formed, but those preferentially aligned with the stress field widen to a larger extent and ultimately accept most of the injected solid material.

Pressure increases until the fracture conductivity and slurry flow matches the flow rate and then stabilizes as illustrated in Figure 11, which is consistent with field observations. Pressure declines after shut-in. A model of small size can simulate one or two injection cycles before fracturing and deformation reaches the boundaries (indicated by little further pressure increase on last injection cycle).

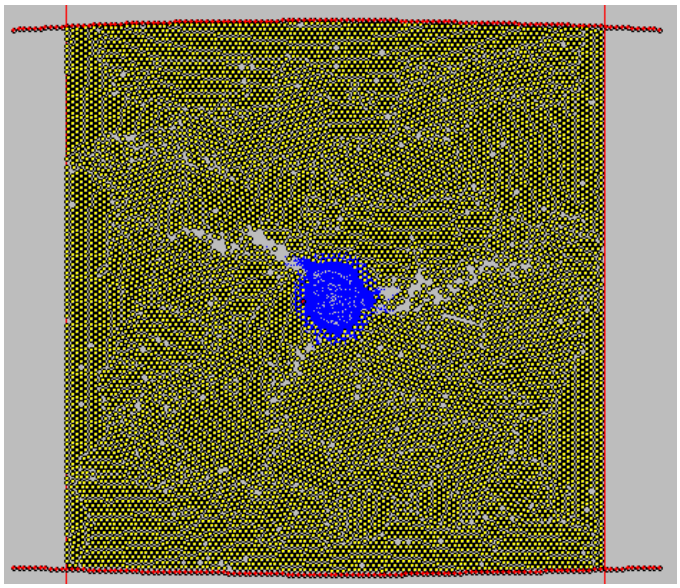

Figure 9. Discrete particle model showing fracture initiation and slurry particle injection

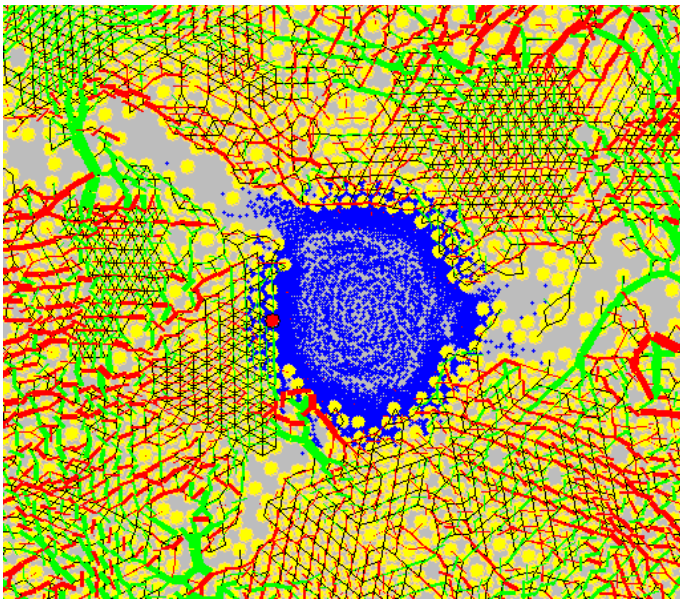

Figure 10. Close-up view of fracture initiation and slurry injection in porous media.

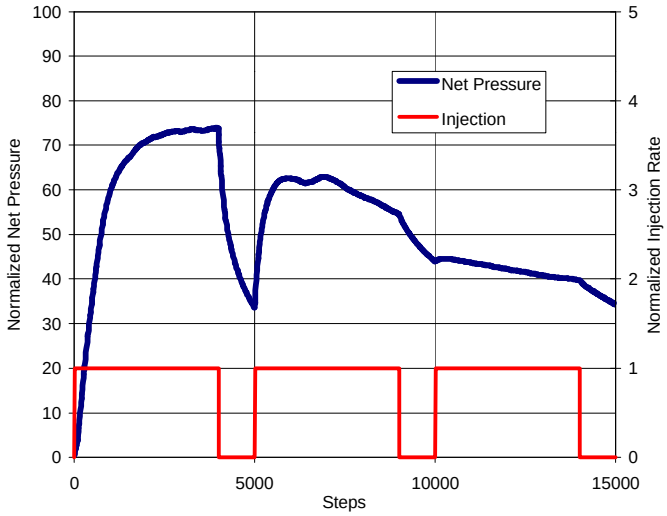

Figure 11. Typical pressure behavior for repeated injection cycles with particle flow model

These preliminary simulation results appear to capture the physical processes involved in solids injection into weakly cemented media. This method shows good potential for better simulating waste injection, and warrants additional investigation and development efforts. For example, the model shown in Figure 7 is limited in size and needs to be expanded by at least a factor of ten to eliminate edge effects and allow simulation of repeated injection episodes. Current efforts are underway with coupled particle and flow model assemblies about ten times larger than those described in this paper, representing a near wellbore region of about 2m x 2m in cross section.

4. CONCLUSIONS

We have investigated the use of coupled fluid flow and particle flow models to simulate fracture and dilation processes during waste injection. These studies lead us to conclude that when formations are weakly cemented with limited shear strength, there is a transition from brittle, discrete fracture extension, to more widescale dilation and inelastic parting. Shear bond strength between particles, rather than tensile bond strength, appears to be the controlling factor on this transition to distributed damage. We were successful in developing a coupling process between a continuum flow model and a discrete particle model, allowing simulation of slurry particle injection and resulting fracture and dilation. These simulation results appear to capture the physical processes involved in solids injection into weakly cemented media, including development of a distributed damage zone around the parting plane. Injected slurry volume is accommodated not simply within the fracture, but within the adjacent porespace through invasion and porosity reduction. Such mechanisms are consistent with laboratory and field observations involving large volume waste injection in unconsolidated media.

ACKNOWLEDGEMENTS

The research described in this paper was funded in part by Terralog Technologies Inc., the Alberta Department of Energy, and the US Department of Energy (contract DE-AC26-99BC1522). We gratefully acknowledge technical support and useful discussions with Mr. William Good, Mr. John Ford, Mr. Alex Reed, and Ms. Susanne Olmstead.

REFERENCES

Bathurst, R.J. & Rothenburg, L. 1990, Observations on stress-force-fabric relationships in idealized granular media., *Mech. of Mat.* 9: 31-48.

Bear, J. 1972, *Dynamics of fluids in porous media*, Environmental Sicence Series, American Elsevier, New York, Reprinted Dover Publications, Inc, 1988

Bruno, M.S. 1994, Micromechanics of stress-induced permeability anisotropy and damage in sedimentary rock, *Mech. of Mat.* 18: 31-48.

Bruno, M.S., Bovberg, C.A. & Meyer, R.F. 1996, Some influences of saturation and fluid flow on sand production: laboratory and discrete element model investigations, SPE 36534 in *Proc. SPE Ann. Tech. Conf. Exh.*, Denver, Colorado, 6-9 October, 1996

Bruno, M.S. & Nakagawa, F.M. 1991, Pore pressure influence on tensile fracture propagation in sedimentary rock, *Int. J. Rock Mech. Min. Sci. & Geomech. Abstr.* 28(1): 261-273.

Bruno, M.S., Reed, A., Olmstead, S. 2000, Environmental management, cost management, and asset management for high-volume oil field waste injection projects, *Proc. IADC/SPE Drilling Conference*, New Orleans, Louisiana, 23-25 February, 2000.

Cleary, M.P. 1979, Rate and structure sensitivity in hydraulic fracturing of fluid-saturated porous formations, *Proc. 20th U.S. Rock Mech. Symp*, Austin, TX

Cundall, P.A. & Strack, O.D.L. 1979, A discrete numerical model for granular assemblies, *Geotechnique*, 29: 47-65.

Griffith, A.A. 1921, The phenomena of rupture and flow in solids, *Phil. Trans. R. Soc.* A221: 163-198.

Irwin, G.R. 1948. "Fracture Dynamics" in *Fracturing of Metals*: 147-166, American Society for Metals, Cleveland.

Irwin, G.R. 1957. Analysis of stresses and strains near the end of a crack traversing a plate, *J. Appl. Mech*, 24: 361-364.

Itasca Consulting Group, Inc. 1996, FLAC, Theory and User Manual, Version 3.3, Itasca Consulting Group Inc. Minnesota

Itasca Consulting Group, Inc. 1999, PFC Theory and Background, Version 2.0, Itasca Consulting Group Inc. Minnesota

Kannenen, M.F. & Popelar, C.H. 1985, *Advanced Fracture Mechanics:* 158-168. Oxford University Press, New York.

Orowan, E. 1948. Fracture and strenth of solids, *Reports on Progress in Physics*, XII: 185

Rice, J.R. 1968, "Mathematical Analysis in the Mechanics of Fracture" in *Fracture*, H. Liebowitz (ed), Academic Press, New York.

Willson, S.M., Steiger, R.P., Moschovidis, Z.A., Abou-Sayed, A.S., Bree, Ph.de & Sirevag, G. 1999, Laboratory investigation of drill cuttings disposal by downhole Injection, *Proc. 37th U.S. Rock Mech. Symp* : 1009-1016, Vail, Colorado, 6-9, 1999